Modulation of Atlantic Basin Tropical Cyclone Activity by the Madden–Julian Oscillation (MJO) from 1905 to 2011

PHILIP J. KLOTZBACH

Department of Atmospheric Science, Colorado State University, Fort Collins, Colorado

ERIC C. J. OLIVER

Institute for Marine and Antarctic Studies, University of Tasmania, and Australian Research Council Centre of Excellence for Climate System Science, Hobart, Australia

(Manuscript received 22 July 2014, in final form 19 September 2014)

ABSTRACT

The Madden–Julian oscillation (MJO) has been demonstrated to play a role in tropical cyclone (TC) activity around the globe in a number of recent studies. While the impact of the MJO on TCs in the Atlantic basin since the mid-1970s has been well documented, a newly developed 107-yr-long index for the MJO allows for additional analysis of the impacts of the MJO on Atlantic TC activity. TC activity in the Atlantic increases when MJO-related convection is enhanced over Africa and the Indian Ocean, while TC activity in the Atlantic is suppressed when the MJO enhances convection over the western Pacific. This long-term record of the MJO also allows for the analysis of how the MJO's impacts may be modulated by other climate modes, such as the El Niño–Southern Oscillation (ENSO) over interannual time scales and the Atlantic multidecadal oscillation (AMO) over multidecadal time scales. When climatologically unfavorable conditions such as an El Niño event or a negative AMO phase are present, even TC-favorable MJO conditions are not enough to generate statistically significant increases in TC activity from the long-term average across the Atlantic basin. However, climatologically favorable conditions during a La Niña event or a warm AMO phase act to enhance the modulation of TC activity over the Atlantic basin by the MJO.

1. Introduction

The Madden–Julian oscillation (MJO), a quasi-oscillatory phenomenon with a convective signal that often originates in the tropical Indo-Pacific and propagates around the equator with a time scale between 30 and 70 days (Madden and Julian 1971, 1972), has been shown to impact tropical cyclone (TC) activity in all ocean basins (Camargo et al. 2009; Klotzbach 2014; and references therein). This impact has been tied to modulations by the MJO of climate fields that are known to impact TC activity (e.g., vertical wind shear, vertical motion, low-level and midlevel moisture, and relative vorticity) (Gray 1968). In fact, the MJO is one of the likely reasons why TCs have been observed to cluster in time (Gray 1979).

The impact of the MJO on North Atlantic TCs has been well documented. Maloney and Hartmann (2000) showed that Gulf of Mexico and western Caribbean Sea hurricane genesis was 4 times more likely to occur when low-level eastern Pacific winds associated with the MJO were westerly than when they were easterly. Barrett and Leslie (2009) showed that enhanced upper-tropospheric divergence was an important driver of hurricane formation in the Atlantic. When MJO-related convection was of a heightened magnitude at 120°W, hurricanes [1-min maximum sustained winds greater than 63 kt ($1\,\text{kt} \approx 0.51\,\text{m s}^{-1}$)] and major hurricanes (1-min maximum sustained winds greater than 95 kt) were 4 times more likely to make landfall than when convection was suppressed in this region. Klotzbach (2010) primarily focused on TCs forming in the main development region (MDR; 7.5°–22.5°N, 75°–20°W) and showed that major hurricane formation in the Atlantic MDR was favored when convection was enhanced over Africa and the western Indian Ocean. Ventrice et al. (2011) found similar results when examining African easterly wave

Corresponding author address: Philip J. Klotzbach, Department of Atmospheric Science, Colorado State University, 200 West Lake Street, 1371 Campus Delivery, Fort Collins, CO 80523.
E-mail: philk@atmos.colostate.edu

DOI: 10.1175/JCLI-D-14-00509.1

activity and TC genesis likelihood in the Atlantic basin. These studies demonstrated approximately 3:1 ratios between major hurricane development and accumulated cyclone energy (ACE) generation (Bell et al. 2000) when the MJO's convective enhancement is located over Africa and the western Indian Ocean, compared with when it is located over the western Pacific. Statistically significant differences in vertical wind shear, midlevel moisture and vertical motion all appear to be contributors to this observed difference in TC formation.

The aim of this paper is to examine the relationship between the MJO and Atlantic TCs over a longer time period than has been possible previously. This can be accomplished using a long historical reconstruction of the Wheeler and Hendon (2004) MJO index over the 1905–2011 period (Oliver and Thompson 2012). The object of this analysis is to examine the stability of the MJO–Atlantic TC relationship over multidecadal time scales, with a much longer time period than is possible using only the Wheeler and Hendon MJO index (which extends back only to 1974).

This paper is organized as follows: Section 2 describes the data utilized in this paper. Section 3 examines both MJO-related modulations of large-scale atmospheric fields across the tropics as well as variations in Atlantic TC activity using both the Wheeler and Hendon (2004) MJO index over 1979–2011 and the extended MJO index of Oliver and Thompson (2012) over the same period. Section 4 then examines the stability of the MJO–Atlantic TC relationships over the earlier part of the twentieth century from 1905 to 1978. Examinations of how the strength of the MJO–Atlantic TC relationship are modulated by El Niño–Southern Oscillation (ENSO; Rasmusson and Carpenter 1982) and by the Atlantic multidecadal oscillation (AMO; Goldenberg et al. 2001) are presented in section 5. A discussion and conclusions are presented in section 6.

2. Data sources

In this paper, we characterize the MJO using two indices. The first is the Wheeler–Hendon (WH) MJO index (Wheeler and Hendon 2004), which combines 200- and 850-mb zonal winds and outgoing longwave radiation (OLR) using a multivariate EOF analysis in order to extract the MJO signal, after removing the annual mean and ENSO-related variability in order to focus on intraseasonal time scales. The resulting real-time multivariate MJO (RMM) time series are then normalized to have a standard deviation of one over the 1979–2001 period. This index is available from 1974 to the present (with an absence of data for most of 1978 because of incomplete OLR observations).

We also used a recently developed reconstruction of the MJO index over the time period 1905–2011 in order to examine relationships with Atlantic basin TCs over longer time scales. This index was developed by Oliver and Thompson (2012) using a multiple linear regression of surface pressures from the Twentieth Century Reanalysis (Compo et al. 2011) onto the Wheeler–Hendon MJO index to reconstruct both components of the RMM time series prior to 1974. This index was normalized to have a standard deviation of one over the 1905–2008 period. For the remainder of the paper, this index will be referred to as the OT MJO index. The index removes the mean over the previous 120 days, which eliminates significant levels of interannual variability along with much of the convective signal associated with ENSO when substantial temporal trends in these signals are absent. Oliver and Thompson (2012) demonstrate good agreement with the Wheeler–Hendon index over the 1979–2008 period. They also show robust relationships with other phenomena known to be closely related to the MJO, such as zonal surface winds and cloud cover in the tropics, intense rainfall over Australia and sea level in the western Pacific (Oliver and Thompson 2012) as well as surface air temperatures over Alaska (Oliver 2014).

Table 1 displays the strength of the MJO (as measured by mean amplitude, median amplitude, and percentage of days where the index exceeds one standard deviation) for the OT index over three time periods: 1905–47, 1948–78, and 1979–2011 and compares them with the same statistics for the WH index over the 1979–2011 period. (The reasons for selecting these three time periods for the OT index are discussed in the following paragraph.) The MJO has a slight positive trend as defined by the OT index over the course of the twentieth century, but this increase is slight and should not impact the results of this paper significantly. In fact, the proportion of time spent above an amplitude of one does not change appreciably among the two indices and three time periods (Table 1). The amplitude of the OT and WH index is virtually the same from 1979 to 2011. It should be noted that both of these indices are statistical approximations to the state of the MJO and therefore cannot be expected to fully capture the dynamics of the MJO but are quite useful for bulk statistical analyses such as those conducted here. Several reanalysis datasets are utilized to characterize the large-scale climate fields. For the time period from 1905 to 1947, we use the Twentieth Century Reanalysis (Compo et al. 2011). This reanalysis was defined on a 2° latitude by 2° longitude grid; assimilates surface pressure, sea level pressure, sea surface temperature, and sea ice data; and then utilizes an ensemble Kalman filter and an ensemble of weather

TABLE 1. Mean amplitude, median amplitude, and percentage of days for which the MJO indices exceed one. These statistics are shown for the OT index over the 1905–47, 1948–78, and 1979–2011 periods and for the WH index over the 1979–2011 period.

	OT (1905–47)	OT (1948–78)	OT (1979–2011)	WH (1979–2011)
Mean amplitude	1.18	1.26	1.31	1.26
Median amplitude	1.09	1.15	1.22	1.17
Percentage of days where amplitude >1	56%	59%	62%	61%

forecasts from a global numerical weather prediction model to arrive at a best estimate of the state of the atmosphere. We also utilize the Twentieth Century Reanalysis for all vertical shear figures. For the time period from 1948 to 1978, for the data in our tables, we use the National Centers for Environmental Prediction–National Center for Atmospheric Research (NCEP–NCAR) reanalysis (Kistler et al. 2001). This reanalysis was defined on a 2.5° latitude by 2.5° longitude global grid and utilizes three-dimensional variational data assimilation to arrive at its estimate of the background state at a specific time. For the time period from 1979 to 2011, we use the European Centre for Medium-Range Weather Forecasts (ECMWF) Interim Re-Analysis (ERA-Interim; Dee et al. 2011). This reanalysis was created on a 1.5° latitude by 1.5° longitude global grid and utilizes four-dimensional variational data assimilation to arrive at its estimate of the background state at a specific time. In addition, we analyze OLR from the National Oceanic and Atmospheric Administration (NOAA) interpolated OLR product (Liebmann and Smith 1996). This product is available on a 2.5° latitude by 2.5° longitude global grid and covers the period 1974–2013 (we utilize OLR data only over the period 1979–2011 in this paper).

Atlantic basin TC activity statistics are calculated from the second-generation hurricane database (HURDAT2; Landsea and Franklin 2013). HURDAT2 provides 6-hourly estimates of location and maximum sustained wind for every TC in the Atlantic basin since 1851, with reanalyzed statistics (as part of the HURDAT2 reanalysis project) over the period from 1905 to 1945 included in this study. ACE will typically be utilized as the metric for TC activity in this paper. It is calculated by squaring the maximum 1-min sustained wind speed in knots at each 6-hourly interval where a TC is at least at tropical storm strength according to the National Hurricane Center and then dividing by 10 000.

The multivariate ENSO index (MEI) is utilized to characterize ENSO for each TC season (Wolter and Timlin 1998). In general, the MEI is considered to be a more robust measure of the atmospheric and oceanic response to ENSO than simply using a sea surface temperature (SST) index. For example, there may be cases where the Niño 3.4 SST index indicates a weak El Niño is present, but the associated Walker circulation shift and weakening is limited. The MEI overcomes this limitation by including SST, sea level pressure, zonal and meridional winds, cloudiness, and surface temperature from the International Comprehensive Ocean–Atmosphere Data Set (ICOADS; Woodruff et al. 2011). We also use the extended MEI (Wolter and Timlin 2011) to characterize ENSO for the period from 1905 to 1949. The extended MEI utilizes SST from the Second Hadley Centre Sea Ice and Sea Surface Temperature dataset (HadSST2; Rayner et al.

TABLE 2. July–October-averaged anomalies of 200-mb U, 850-mb U, 200-mb U − 850-mb U (vertical shear), SST, SLP (1 mb = 1 hPa), OLR, 300-mb ω, and 700-mb RH in the North Atlantic MDR (7.5°–22.5°N, 75°–20°W) between 1979 and 2011 using ERA-Interim. Anomalies are calculated as deviations from the MJO index phase 1–8 average when the WH MJO index is greater than one. Values that are significantly different at the 1% level from the phase 1–8 average in a TC-favorable manner are highlighted in boldface type, whereas differences that are significant at the 1% level from the phase 1–8 average in a TC-unfavorable manner are highlighted in boldface and italics.

MJO index phase	200-mb U ($m\,s^{-1}$)	850-mb U ($m\,s^{-1}$)	200-mb U − 850-mb U ($m\,s^{-1}$)	SST (°C)	SLP (mb)	OLR ($W\,m^{-2}$)	300-mb ω ($mb\,day^{-1}$)	700-mb RH (%)
1	**−0.85**	0.04	**−0.89**	***−0.04***	**−0.50**	**−1.67**	**−1.85**	0.00
2	**−1.93**	**0.61**	**−2.54**	**0.12**	**−0.50**	**−3.85**	**−4.85**	**1.51**
3	**−1.69**	**0.34**	**−2.03**	0.07	***0.29***	0.77	0.51	0.83
4	0.05	**0.22**	−0.17	**0.20**	***0.18***	***2.81***	***2.27***	0.29
5	***1.58***	−0.07	***1.65***	0.13	***0.28***	***0.69***	0.53	0.26
6	***1.94***	***−0.60***	***2.54***	***−0.12***	***0.42***	***1.17***	***2.50***	***−1.55***
7	***2.77***	***−0.97***	***3.74***	***−0.25***	***0.29***	−0.42	0.76	***−1.76***
8	***2.20***	−0.18	***2.38***	0.00	**−0.57**	−1.19	−0.36	−0.65

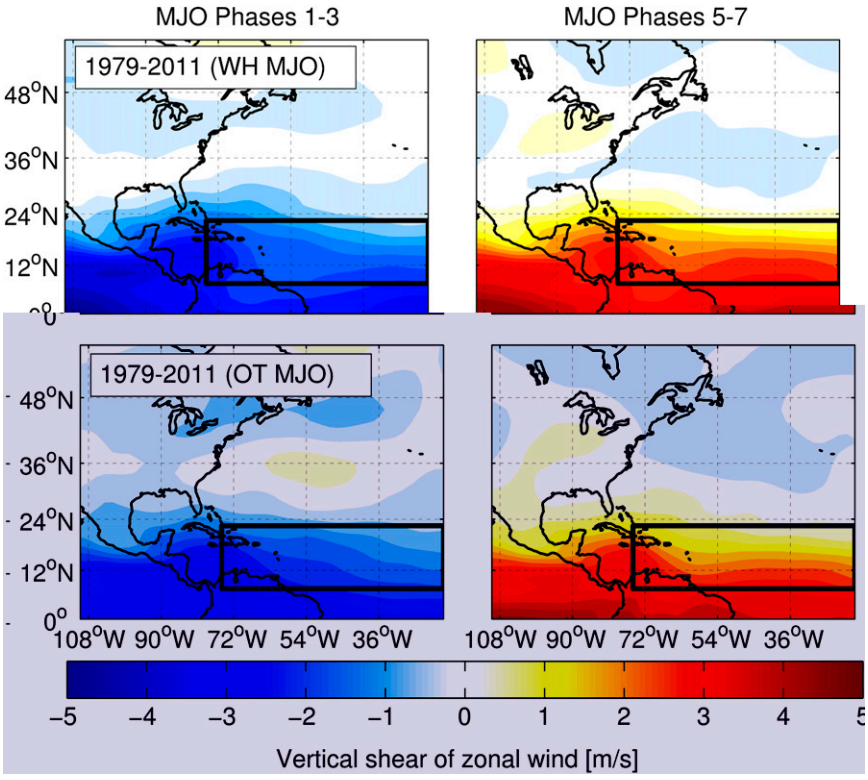

FIG. 1. Zonal vertical shear anomalies (200-mb U − 850-mb U) for all days where the WH MJO index exceeded an amplitude of one for (top left) MJO index phases 1–3 and (top right) MJO index phases 5–7. Also displayed are zonal vertical shear anomalies for all days where the OT MJO index exceeded an amplitude of one for (bottom left) MJO index phases 1–3 and (bottom right) MJO index phases 5–7.

2006) and surface pressure from the Second Hadley Centre Sea Level Pressure dataset (HadSLP2; Allan and Ansell 2006). Both the extended MEI and the MEI are computed using a bimonthly average. The MEI value over the Atlantic TC season is calculated as the average of July–August, August–September, and September–October values. If the MEI is greater (less) than or equal to 0.75 (−0.75), an El Niño (La Niña) event is defined; all times for which values lie between −0.75 and 0.75 are defined as neutral events.

The AMO is characterized by a horseshoe-shaped SST pattern in the North Atlantic (Goldenberg et al. 2001). Positive phases generally have warm water anomalies in the tropical and subpolar North Atlantic, while negative phases have opposite-signed SST anomalies. Positive and negative AMO periods are as defined using the phases discussed by Klotzbach and Gray (2008), with the recent positive period defined in their analysis extended to include up to 2011. Namely, we define 1926–69 and 1995–2011 as positive AMO phases and 1905–25 and 1970–94 as negative AMO phases.

TABLE 3. As in Table 2, but for the OT MJO index using ERA-Interim from 1979 to 2011.

MJO index phase	200-mb U (m s^{-1})	850-mb U (m s^{-1})	200-mb U − 850-mb U (m s^{-1})	SST (°C)	SLP (mb)	OLR (W m^{-2})	300-mb ω (mb day^{-1})	700-mb RH (%)
1	**−1.27**	0.18	**−1.45**	−0.05	**−0.51**	−0.70	−1.45	0.61
2	**−1.83**	**0.47**	**−2.31**	0.03	**−0.24**	**−2.44**	**−2.66**	**1.04**
3	**−1.33**	**0.43**	**−1.76**	0.05	***0.26***	−0.20	**−1.56**	**0.98**
4	−0.01	**0.47**	**−0.48**	**0.15**	0.15	0.94	0.97	**1.23**
5	1.01	***−0.27***	***1.28***	0.01	***0.62***	***2.72***	***2.63***	***−1.10***
6	***2.66***	***−0.60***	***3.26***	***−0.08***	***0.38***	0.72	1.22	***−0.78***
7	***2.92***	***−0.63***	***3.55***	0.01	−0.25	−1.39	−0.58	0.26
8	***2.97***	−0.08	***3.05***	−0.01	**−0.61**	**−1.99**	−0.85	−0.45

3. Comparison of WH MJO index and OT MJO index from 1979 to 2011

Climate anomaly fields over the period from 1979 to 2011 were calculated from ERA-Interim. We examined several large-scale fields that are known to impact TCs and have been used in previous MJO modulation studies (e.g., Klotzbach 2010, 2014): SST, sea level pressure (SLP), 850-mb zonal wind (U), 200-mb U, vertical shear of U (defined as 200-mb U minus 850-mb U), 700-mb relative humidity (RH), 300-mb vertical velocity (ω), and OLR. Anomalies were defined as MJO composite averages for each of the eight MJO index phases (for MJO amplitudes greater than one) and calculated from the 1979–2011 climatology during the months of July–October over the Atlantic MDR, which is defined as 7.5°–22.5°N, 75°–20°W.

Table 2 displays climate anomalies for each of the eight MJO index phases using the WH MJO index. Conditions that are known to be favorable for TC formation include above-average SSTs, below-average SLPs, below-average vertical wind shear, above-average vertical motion, and above-average midlevel moisture (Gray 1968). Anomalous easterly flow at upper levels and anomalous westerly flow at lower levels counteracts the prevailing zonal winds across the tropical Atlantic Ocean and Caribbean Sea, thereby reducing the vertical wind shear. Features that are significant at the 1% level in a TC-favorable manner from the phase 1–8 average are highlighted in boldface, while features that are significant at the 1% level in a TC-unfavorable manner are

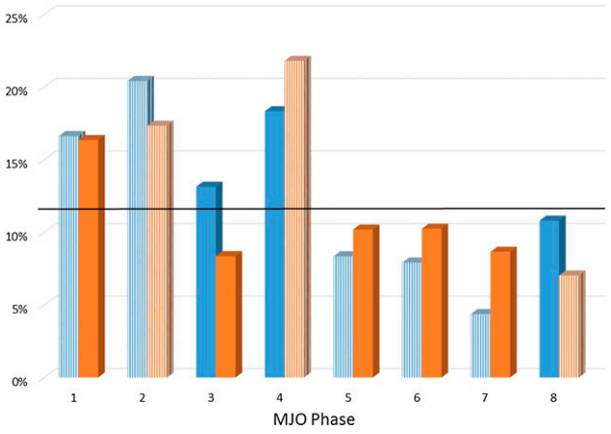

FIG. 2. Percentage of total normalized ACE generated by TCs forming in each phase of the MJO for both the WH MJO index (blue columns) and OT MJO index (orange columns) over the 1979–2011 period. Statistically significant differences at the 10% level are highlighted with vertical striping. The black line denotes the null hypothesis of 12.5% of ACE generated in each of the eight MJO index phases.

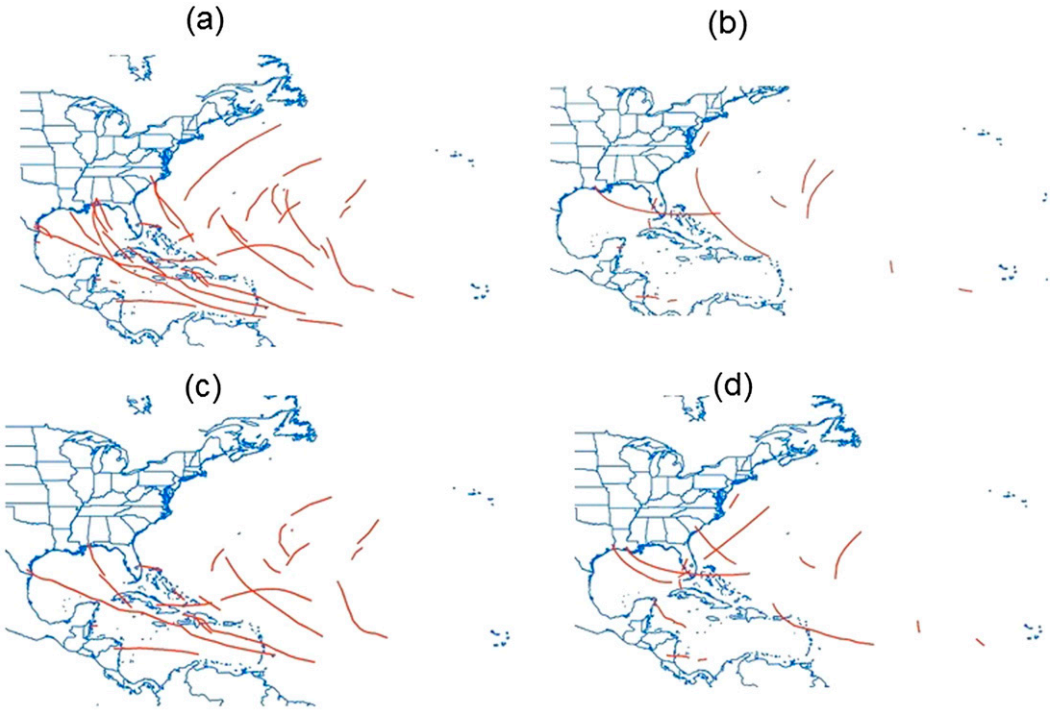

FIG. 3. Tracks of major hurricanes for all days where the WH MJO index exceeded an amplitude of one for (a) MJO index phases 1–3 and (b) MJO index phases 5–7. Also displayed are tracks of major hurricanes for all days where the OT MJO index exceeded an amplitude of one for (c) MJO index phases 1–3 and (d) MJO index phases 5–7.

TABLE 4. As in Table 2, but for the period from 1948 to 1978 as calculated from the NCEP–NCAR reanalysis using the OT MJO index. OLR is not available prior to 1974 and consequently is not displayed in this table.

MJO index phase	200-mb U ($m\,s^{-1}$)	850-mb U ($m\,s^{-1}$)	200-mb U − 850-mb U ($m\,s^{-1}$)	SST (°C)	SLP (mb)	300-mb ω ($mb\,day^{-1}$)	700-mb RH (%)
1	**−0.87**	**0.21**	**−1.08**	0.01	**−0.36**	**−1.96**	**0.85**
2	**−1.19**	**0.68**	**−1.87**	−0.02	**−0.22**	−0.48	0.33
3	0.78	**0.54**	0.23	0.06	**−0.24**	0.01	0.17
4	0.24	***−0.26***	0.50	−0.03	***0.49***	***3.03***	−0.74
5	0.90	***−0.40***	***1.30***	−0.04	***0.60***	0.61	***−0.87***
6	1.13	***−0.27***	1.41	**0.11**	***0.20***	−0.51	−0.61
7	***1.85***	−0.19	***2.05***	0.08	−0.22	−0.34	−0.84
8	***2.04***	−0.18	***2.22***	−0.02	**−0.51**	**−2.83**	−0.01

highlighted in boldface and italics. Significance levels are determined using a bootstrap resampling technique from the full time series of anomalies (Efron 1979). A total of the number of days that the MJO was greater than one for each MJO index phase are selected randomly with replacement from the full sample 10 000 times, and anomalies with a magnitude that occurs fewer than 1% of the time in the random sample are considered to be statistically significant. This same significance test has been conducted for all climate field anomalies displayed here.

As was shown by Klotzbach (2010), the WH MJO index generally shows favorable TC formation conditions in phases 1–3, while unfavorable TC formation conditions are observed in phases 5–7. Differences in 200- and 850-mb U (referred to as vertical shear) among various phases of the MJO are quite notable, with differences in shear anomalies between phases 2 and 7 exceeding 6 $m\,s^{-1}$. Maps of shear anomalies (Fig. 1, top) indicate large deviations over the tropical Atlantic generally and the MDR specifically, with strong negative (positive) values in phases 1–3 (5–7) as the MJO propagates through the domain. Vertical motion differences, as indicated by 300-mb ω, as well as OLR are also observed to vary in a statistically significant manner (Table 2). RH modulations are relatively small over the Atlantic MDR based on the WH MJO index, similar to that shown by Klotzbach (2010). While these RH anomalies are small, they may still be important for modulation of Atlantic basin TC genesis and intensification, as discussed by Camargo et al. (2009).

Table 3 displays similar climate field calculations over the MDR but for the OT MJO index. Significant differences in vertical wind shear are observed in a manner that is consistent with the results using the WH MJO index. Maps of shear anomalies (Fig. 1, bottom) indicate large deviations with the same general pattern and magnitude as was observed for the WH MJO index. Phases 1–3 of the OT MJO index tend to be characterized by TC-enhancing conditions, with phases 5–7 characterized by TC-suppressing conditions, consistent with the results using the WH MJO index. Phase 8 has an interesting combination of statistically significantly favorable thermodynamic conditions (SLP and OLR) and unfavorable dynamic conditions (vertical shear). In general, the modulation of large-scale fields is slightly stronger for the WH index than for the OT index. This is perhaps not surprising, given that the WH index is defined explicitly using OLR and upper- and lower-level zonal winds while the OT index reconstructs the WH index variability using surface pressures alone.

We expect to see similar MJO modulations of TC activity in the Atlantic basin between the WH MJO and OT MJO indices given the broadly similar climate conditions observed for the eight MJO index phases. As was done by Klotzbach (2010), we tabulate TC statistics for a storm based on the phase and amplitude of the MJO on the day that a TC was first classified as a named storm by the National Hurricane Center. Only TCs that formed when the MJO amplitude was greater than one are counted in this analysis. Normalized ACE is calculated following Klotzbach (2010). Namely, the total ACE generated in each MJO index phase is calculated, divided by the number of days that the MJO is in a particular phase, and multiplied by 100. Normalization is important, as the MJO does not spend the same amount of time in each of the eight MJO phases. Figure 2 displays the percentage of normalized ACE generated in each of the eight phases of the MJO for both the WH MJO and the OT MJO. If the MJO did not have any effect on TC activity levels, we would expect to see 12.5% of TC activity generated in each of the eight phases. Statistically significant differences in TC activity at the 10% level, calculated using a 10 000 member bootstrap resampling technique, were highlighted with vertical striping. This same significance test was conducted for all TC statistics displayed here. While statistical significance thresholds were reached for somewhat different MJO index phases for the WH MJO versus the OT MJO indices, the broad pattern of enhanced TC activity in MJO

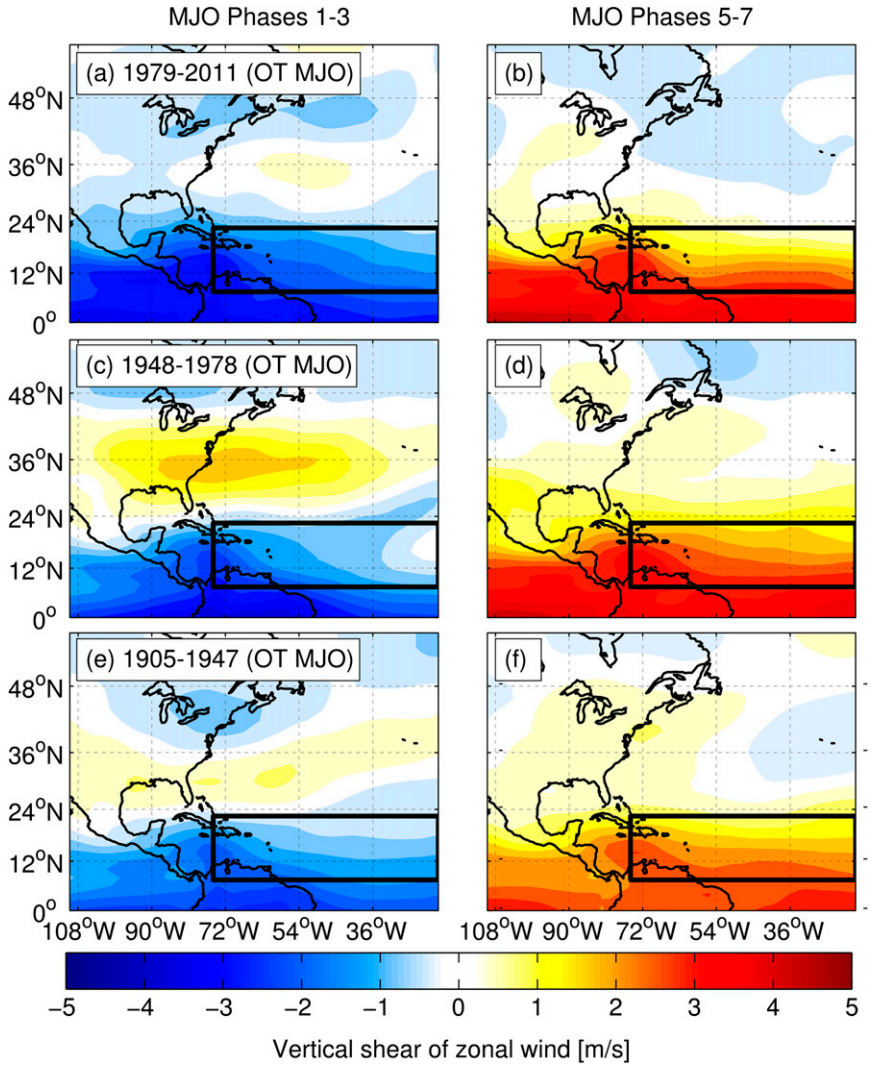

FIG. 4. Zonal vertical shear anomalies (200-mb U − 850-mb U) for all days where the OT MJO index exceeded an amplitude of one for (a) MJO index phases 1–3 and (b) MJO index phases 5–7 for 1979–2011 (as in Fig. 1, bottom). Also displayed are zonal vertical shear anomalies for all days where the OT MJO index exceeded an amplitude of one for (c) MJO index phases 1–3 and (d) MJO index phases 5–7 for 1948–78 and for (e) MJO index phases 1–3 and (f) MJO index phases 5–7 for 1905–47.

index phases 1–4 and suppressed TC activity MJO index phases 5–8 held for both indices.

Figures 3a and 3b display the tracks of major (Saffir–Simpson scale categories 3–5) hurricanes using the WH MJO index for MJO index phases 1–3 and MJO index phases 5–7, respectively. Large differences in the number of normalized major hurricanes are observed over the period from 1979 to 2011 with the WH MJO index, with ratios of 2.5:1 for major hurricanes and 3.9:1 for major hurricane days between MJO index phases 1–3 and MJO index phases 5–7, respectively. As will be shown in the next section, the MJO modulation of TCs during phases 4 and 8 is not stable over the entire 1905–2011 period.

Figures 3c and 3d display tracks of major hurricanes for MJO index phases 1–3 and MJO index phases 5–7, respectively, but using the OT MJO index over the period from 1979 to 2011. Ratio differences for normalized major hurricanes and normalized major hurricane days between MJO index phases 1–3 and MJO index phases 5–7, respectively, are 2.1:1 for major hurricanes and 1.8:1 for major hurricane days. Given the robustness of the relationships between MJO index phases and TC indices demonstrated above, we are motivated to examine the relationship between the OT MJO index and Atlantic basin TC activity over the earlier part of the twentieth century (prior to 1979).

4. Evaluation of the OT MJO index from 1905 to 1978

We next evaluate the MJO–Atlantic TC relationship over two separate time periods during the earlier part of the twentieth century using the OT MJO index: 1948–78 (section 4a) and 1905–47 (section 4b). The dates for these two time periods were selected based upon the availability of the NCEP–NCAR reanalysis, which began in 1948, and the earliest date for which we have an estimation of MJO activity from the OT MJO index, which is 1905.

a. 1948–78

We now evaluate the OT MJO–Atlantic TC relationship from 1948 to 1978 using the NCEP–NCAR reanalysis. Table 4 displays climate field modulations from 1948 to 1978 in a similar manner to Tables 2 and 3, with the exception that no data are displayed for OLR (only available since 1974). As was the case when examining the recent period from 1979 to 2011, similar MJO-generated modulations were observed during the 1948–78 period, with zonal shear differences between MJO index phases 1–3 and MJO index phases 5–7 approaching 4 m s^{-1} (Figs. 4c,d). Note also the consistency in shear modulation between the 1948–78 period and the 1979–2011 period (Figs. 4a,b), as well as the 1905–47 period (Figs. 4e,f). Phase 8 continues to be characterized by a combination of favorable thermodynamic but unfavorable dynamic conditions.

The anomaly magnitude of the MJO modulation of TC activity is even greater during the 1948–78 period compared with the 1979–2011 period. Figure 5 displays normalized ACE generated by TCs forming in each phase of the MJO for the three subperiods of 1905–47, 1948–78, and 1979–2011. MJO index phases 1–3 are characterized by heightened levels of TC activity, while phases 5–7 are characterized by reduced levels of activity for the period from 1948 to 1978, broadly similar to what was shown during the period from 1979 to 2011 as well as the earlier period from 1905 to 1947.

Figures 6c and 6d display tracks of major hurricanes in phases 1–3 and phases 5–7 using the OT MJO index over the period from 1948 to 1978, respectively. Note the consistency of the relationship between the 1948–78 period along with the earlier period 1905–47 and the 1979–2011 period. Ratios are considerably larger for major hurricanes and major hurricane days from 1948 to 1978 than from 1979 to 2011. The normalized major hurricane ratio is 4.4:1 and the normalized major hurricane day ratio is 7.9:1 between MJO index phases 1–3 and MJO index phases 5–7, respectively. This result is somewhat surprising, given the increased uncertainty in both observations of TCs as well as the MJO as one goes back in time. We intend to investigate this further in future work.

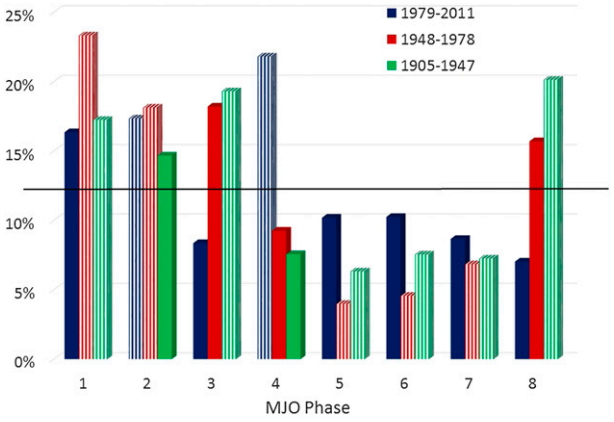

FIG. 5. As in Fig. 2, but for the percentage of normalized ACE generated in each MJO index phase (as defined by the OT index) during the periods 1979–2011 (blue columns), 1948–78 (red columns), and 1905–47 (green columns).

b. 1905–47

We next evaluate the OT MJO–Atlantic TC relationship from 1905 to 1947 using the Twentieth Century Reanalysis for climate anomaly calculations. Table 5 displays modulations over the 1905–47 period. Phases 1–3 continue to be characterized by strongly TC-favorable shear anomalies, while phases 5–7 are characterized by unfavorable shear anomalies (Figs. 4e,f). Phase 8 is characterized by a combination of favorable thermodynamic and unfavorable dynamic conditions, consistent with what was shown for the 1979–2011 and 1948–78 periods.

TC activity modulations continue to show robust differences over the MJO cycle in the 1905–47 period (Fig. 5). The favorable thermodynamic conditions that characterize phase 8 appear to dominate during the early part of the twentieth century, as phase 8 is shown to be the most active TC phase of the MJO. Phases 1–3 continue to be characterized by heightened levels of TC activity, while phases 5–7 are characterized by reduced levels of activity, similar to what was shown for the 1948–78 and 1979–2011 periods. There appears to have been a phase shift over the course of the twentieth century favoring TC development in phase 8 during the early part of the twentieth century. Phase 8 became less favorable over the course of the twentieth century, while phase 4 became progressively more favorable. This phenomenon will be addressed in more detail in section 6.

Figures 6e and 6f display tracks of major hurricanes in phases 1–3 and phases 5–7 using the OT MJO index over the period from 1905 to 1947. The normalized major

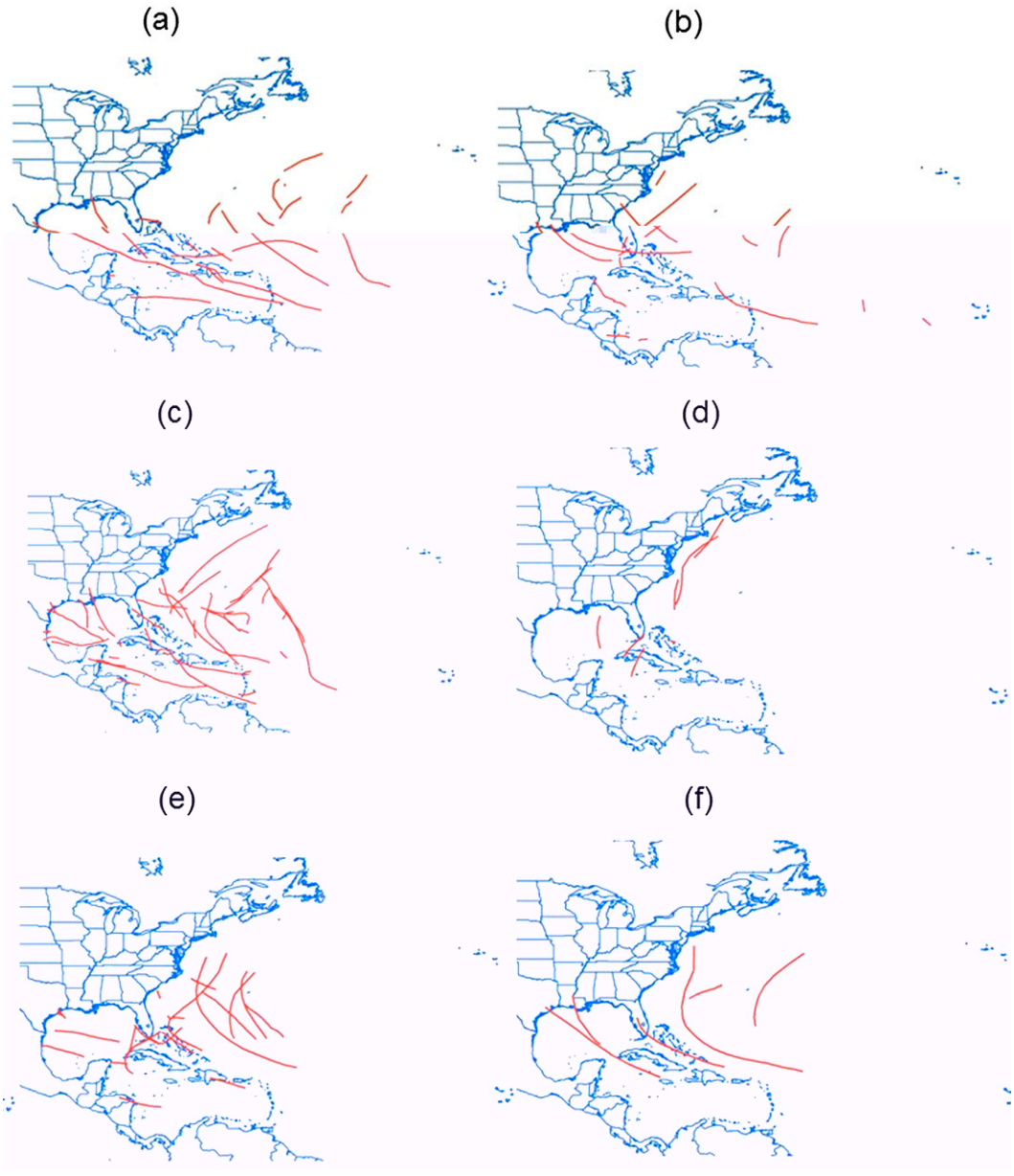

FIG. 6. As in Fig. 3, but for OT MJO index for (a) phases 1–3 from 1979 to 2011, (b) phases 5–7 from 1979 to 2011, (c) phases 1–3 from 1948 to 1978, (d) phases 5–7 from 1948 to 1978, (e) phases 1–3 from 1905 to 1947, and (f) phases 5–7 from 1905 to 1947.

hurricane ratio is 4.2:1 and the normalized major hurricane day ratio is 5.0:1 between MJO index phases 1–3 and MJO index phases 5–7, respectively, which is slightly less than the ratio documented from 1948 to 1978 but greater than the ratio documented from 1979 to 2011.

5. Influence of climate modes

In section 4, we demonstrated the stability of the connection between the MJO and Atlantic TCs over the past 100+ yr of data. We now examine how the MJO's impact on Atlantic basin TCs is modulated by both ENSO and the AMO.

a. ENSO–MJO

The unfavorable influence of El Niño conditions on Atlantic basin TC activity has been shown in a variety of studies, starting with the seminal work of Gray (1984) and in many papers since, including Goldenberg and Shapiro (1996), Tang and Neelin (2004), and Klotzbach (2011). The primary reason that El Niño is typically deemed to be

TABLE 5. As in Table 2, but for the period from 1905 to 1947 as calculated from the Twentieth Century Reanalysis using the OT MJO index. OLR is not available prior to 1974 and consequently is not displayed in this table.

MJO index phase	200-mb U ($m\,s^{-1}$)	850-mb U ($m\,s^{-1}$)	200-mb U − 850-mb U ($m\,s^{-1}$)	SST (°C)	SLP (mb)	300-mb ω ($mb\,day^{-1}$)	700-mb RH (%)
1	**−0.28**	**0.40**	**−0.68**	0.00	**−0.49**	**−2.54**	**0.58**
2	**−1.09**	**0.41**	**−1.50**	***−0.05***	−0.04	−0.62	0.40
3	**−0.99**	**0.66**	**−1.65**	0.06	−0.12	−1.74	**0.95**
4	0.73	0.21	0.52	**0.08**	***0.23***	0.06	0.05
5	0.84	***−0.34***	***1.18***	−0.02	***0.44***	***2.70***	***−0.30***
6	0.96	***−0.27***	***1.22***	***−0.03***	***0.37***	***1.86***	***−0.85***
7	***2.35***	***−0.27***	***2.62***	0.01	−0.24	1.09	***−0.45***
8	***3.21***	0.03	***3.18***	**0.12**	**−0.63**	**−3.06**	0.28

unfavorable to Atlantic TC formation is due to increased upper-level westerly winds attributed to the weakened and eastward-shifted Walker circulation that occurs during El Niño events. These increased upper-level westerly winds thereby increase Atlantic basin vertical shear (Gray 1984). In addition, anomalous upper-tropospheric warming occurs during El Niño events, thereby increasing static stability and suppressing TC formation (Tang and Neelin 2004).

Table 6 displays climate field modulations over the period from 1905 to 2011 using the Twentieth Century Reanalysis during El Niño events. As a reminder, anomalies are calculated with respect to all years. Note that none of the eight MJO index phases are characterized by statistically significantly reduced vertical shear, while six of the eight phases are characterized by statistically significantly stronger than normal vertical shear. None of the eight phases are characterized by enhanced vertical motion, indicative that El Niño creates a more detrimental dynamic and thermodynamic environment that even favorable MJO index phases cannot overcome. It should be noted that the vertical shear anomalies modulated by the MJO are significantly reduced during El Niño events, likely because of the weaker Walker circulation during these years. It appears that it is the modulation of thermodynamic fields such as relative humidity and vertical motion that drives MJO-related TC variability observed in El Niño events.

Table 7 displays climate field modulations by the MJO during La Niña events. Three of the eight MJO index phases are characterized by significantly anomalously weak vertical wind shear, and four of the eight phases are characterized by enhanced vertical motion. The variability in vertical shear modulated by MJO phase is much greater during La Niña events than was observed in El Niño events. As would be expected given the extensive research that has been conducted in the past regarding ENSO's impacts on TC activity, favorable MJO index phases combined with La Niña events generate environments that are quite conducive for TC formation. Figure 7 shows the difference between vertical shear for MJO index phases 1–3 during La Niña events and MJO index phases 5–7 during El Niño events, in order to demonstrate how significant these differences can be.

Figure 8 displays normalized ACE generated in each phase of the MJO conditioned on ENSO events. As would be expected given the overall more favorable basic state in La Niña events, statistically significant TC increases are achieved in phases 1–2, while phases 4–7 have statistically significant decreases in El Niño events. Only phase 5 has a statistically significant decrease in La Niña events, while no phases have a statistically significant increase in El Niño events. All phases of the MJO except for phase 5 have more TC activity in La Niña events. These differences can also be seen by looking at tracks of major hurricanes in MJO index phases 1–3 in

TABLE 6. Climate field modulations for El Niño events over the 1905–2011 period using data from the Twentieth Century Reanalysis and the OT MJO index.

MJO index phase	200-mb U ($m\,s^{-1}$)	850-mb U ($m\,s^{-1}$)	200-mb U − 850-mb U ($m\,s^{-1}$)	SST (°C)	SLP (mb)	300-mb ω ($mb\,day^{-1}$)	700-mb RH (%)
1	***2.19***	**0.64**	***1.55***	**0.09**	**−0.50**	−0.03	**0.75**
2	***1.83***	**0.64**	***1.19***	−0.08	0.18	***3.06***	−0.48
3	***2.25***	0.39	***1.86***	***−0.16***	0.26	2.61	0.43
4	−0.09	***−0.78***	0.69	***−0.21***	***1.24***	***6.60***	***−2.14***
5	−0.33	***−0.63***	0.30	***−0.15***	0.97	***8.52***	***−1.61***
6	0.78	***−1.05***	***1.83***	***−0.09***	***0.92***	***4.71***	***−1.58***
7	***2.14***	***−0.54***	***2.68***	−0.02	0.21	0.84	0.01
8	***4.10***	**0.22**	***3.88***	**0.10**	**−0.58**	−0.02	0.18

TABLE 7. As in Table 6, but for La Niña events.

MJO index phase	200-mb U (m s^{-1})	850-mb U (m s^{-1})	200-mb U − 850-mb U (m s^{-1})	SST (°C)	SLP (mb)	300-mb ω (mb day^{-1})	700-mb RH (%)
1	**−3.45**	−0.01	**−3.44**	***−0.15***	**−0.35**	**−2.95**	0.13
2	**−3.83**	**0.53**	**−4.36**	***−0.14***	**−0.29**	**−2.28**	**0.85**
3	**−2.89**	**0.74**	**−3.63**	−0.02	−0.25	**−2.18**	**1.74**
4	−0.38	**0.28**	−0.66	***0.07***	−0.06	**−3.12**	0.57
5	***2.14***	0.01	***2.13***	***−0.06***	−0.06	0.79	−0.19
6	***2.67***	0.11	***2.56***	−0.02	−0.16	1.08	***−0.97***
7	1.36	0.22	1.15	***−0.13***	**−0.70**	0.19	−0.20
8	−0.20	***−0.71***	0.51	***−0.25***	−0.31	0.03	−0.94

La Niña events compared with tracks of major hurricanes in MJO index phases 5–7 in El Niño events (Fig. 9). During the period from 1905 to 2011, there are 5.3 times as many major hurricanes and 14.2 times as many major hurricane days in MJO index phases 1–3 compared with MJO index phases 5–7 when conditioned on phase of ENSO and normalized by the number of days spent in each MJO index phase during El Niño or La Niña conditions.

b. *AMO–MJO*

We now turn to the combined impacts of the AMO and MJO on TC activity in the Atlantic basin. Positive phases of the AMO are associated with a variety of conditions that are typical of active Atlantic TC seasons, including anomalously warm SSTs, anomalously low sea level pressures, and anomalously weak vertical wind shear (Goldenberg et al. 2001; Klotzbach and Gray 2008). As was done by Klotzbach and Gray (2008), we take positive AMO periods to be 1926–69 and 1995–2011, while negative AMO periods are taken to be 1905–25 and 1970–94.

Table 8 displays anomalies of climate fields during negative AMO years over the 1905–2011 period using the Twentieth Century Reanalysis. Negative AMO years are generally characterized by unfavorable conditions for all MJO index phases, although the impact seems to be more for thermodynamic factors than dynamic factors, in contrast to ENSO's impacts discussed in the previous section. For example, MJO index phases 2 and 3 have significantly weaker vertical shear in negative AMO phases, in contrast to El Niño years where no MJO index phases had significantly weaker vertical shear. Thermodynamics are generally less conducive in negative AMO years, with all eight phases of the MJO displaying significantly cool SST anomalies, along with generally higher SLPs, reduced 700-mb relative humidity levels, and downward vertical motion anomalies.

Climate field anomalies are displayed for positive AMO years in Table 9. Vertical shear anomalies are somewhat more conducive than for negative AMO years, while the thermodynamic environment is much more conducive. All eight phases of the MJO display significantly positive SST anomalies, with generally lower SLPs, moister middle levels, and anomalous upward vertical motion also being experienced when the AMO is positive.

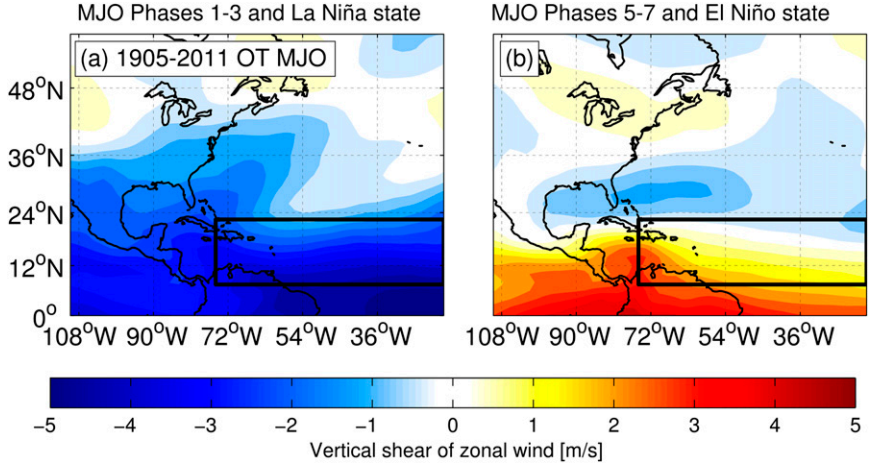

FIG. 7. Zonal vertical shear anomalies (200-mb U − 850-mb U) for all days where the OT MJO index exceeded an amplitude of one for (a) MJO index phases 1–3 and during La Niña events only and (b) MJO index phases 5–7 and during El Niño events only for 1905–2011.

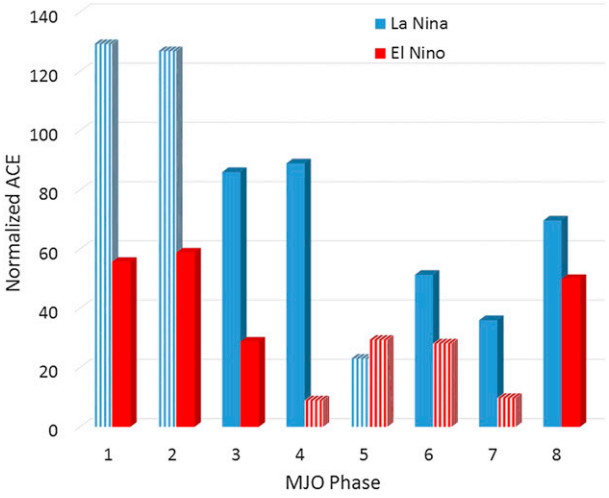

FIG. 8. Normalized ACE generated by each phase of the MJO during La Niña events (blue bars) and El Niño events (red bars). Statistically significant differences at the 10% level are highlighted with vertical striping.

Normalized ACE generated in each phase of the MJO conditioned by AMO phase is displayed in Fig. 10. Given the somewhat more favorable dynamic and significantly more favorable thermodynamic environment during a positive AMO phase, one would expect to see more TC activity in positive AMO phases. Phases 1–4 and 8 experience significant enhancement of ACE in positive AMO phases, while no MJO index phases have a significant enhancement of ACE in negative AMO phases. Phase 5 is characterized by significant suppression of TC activity in both positive and negative AMO phases, while negative AMO phases also significantly suppress TC activity in MJO index phases 4, 6, and 7. Strong relationships are also observed when examining major hurricane tracks (Fig. 11). During the period from 1905 to 2011, there are 3.7 times as many major hurricanes and 4.2 times as many major hurricane days in MJO index phases 1–3 compared with MJO index phases 5–7 when conditioned on phase of AMO and normalized by the number of days spent in each phase of the MJO.

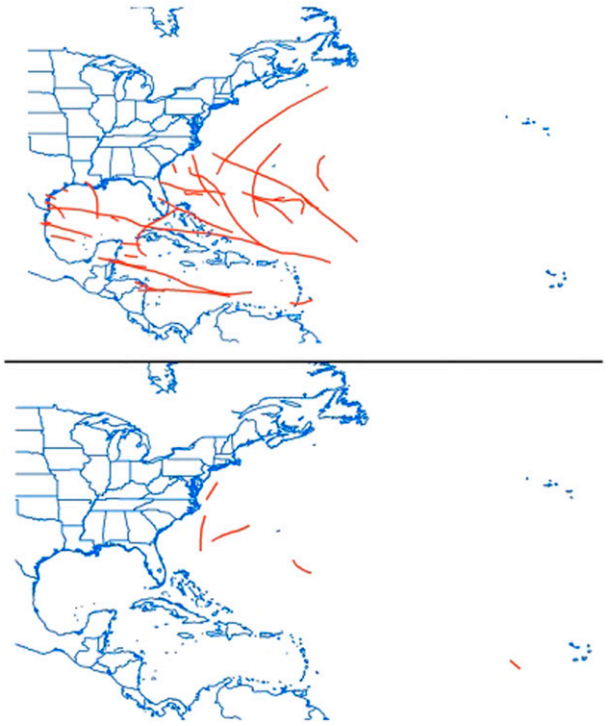

FIG. 9. Major hurricane tracks during (top) MJO index phases 1–3 and La Niña years and (bottom) MJO index phases 5–7 and El Niño years.

6. Discussion and conclusions

This paper is the first to document impacts of the MJO on Atlantic basin TC activity over multidecadal time scales. We find that, over the 1905–2011 period, MJO index phases 1–3 are typically associated with active periods for Atlantic TC activity while MJO index phases 5–7 are typically associated with quiet periods for Atlantic TC activity, similar to what has been documented for more recent time periods (e.g., Klotzbach 2010; Ventrice et al. 2011). This pattern remained remarkably stable over the duration of the twentieth century. Given the long record (1905–2011) of MJO activity available from the OT MJO dataset we then examined the modulation of the MJO–Atlantic TC relationship on interannual and multidecadal time scales by

TABLE 8. As in Table 6, but for negative AMO years.

MJO index phase	200-mb U (m s^{-1})	850-mb U (m s^{-1})	200-mb U − 850-mb U (m s^{-1})	SST (°C)	SLP (mb)	300-mb ω (mb day^{-1})	700-mb RH (%)
1	−0.11	−0.03	−0.08	***−0.19***	***−0.15***	0.51	***−0.49***
2	***−0.87***	***0.19***	***−1.06***	***−0.24***	***0.20***	0.52	−0.19
3	−0.70	***0.23***	***−0.93***	***−0.18***	***0.41***	***2.77***	−0.03
4	0.39	−0.12	0.51	***−0.13***	***0.64***	***3.00***	***−1.06***
5	***1.37***	***−0.52***	***1.89***	***−0.23***	***0.78***	***4.82***	***−1.31***
6	***1.95***	***−0.67***	***2.62***	***−0.24***	***0.59***	***3.27***	***−1.44***
7	***2.26***	***−0.64***	***2.90***	***−0.15***	0.00	***1.14***	−0.45
8	***3.12***	***−0.24***	***3.36***	***−0.17***	***−0.36***	0.15	***−0.87***

TABLE 9. As in Table 6, but for positive AMO years.

MJO index phase	200-mb U ($m\,s^{-1}$)	850-mb U ($m\,s^{-1}$)	200-mb U − 850-mb U ($m\,s^{-1}$)	SST (°C)	SLP (mb)	300-mb ω ($mb\,day^{-1}$)	700-mb RH (%)
1	**−1.15**	**0.43**	**−1.57**	**0.15**	**−0.72**	**−4.70**	**1.16**
2	**−1.50**	**0.67**	**−2.17**	**0.12**	**−0.39**	**−3.08**	**1.04**
3	−0.69	**0.76**	**−1.45**	**0.19**	**−0.30**	**−3.51**	**1.33**
4	−0.41	**0.45**	−0.86	**0.23**	−0.03	**−1.84**	**0.68**
5	0.32	***−0.23***	0.55	**0.16**	***0.38***	***2.05***	−0.09
6	***1.20***	−0.16	***1.36***	**0.19**	0.13	0.75	−0.05
7	***2.24***	0.05	***2.19***	**0.16**	**−0.43**	0.05	0.46
8	***2.45***	**0.25**	***2.20***	**0.24**	**−0.90**	**−4.20**	**1.23**

ENSO and the AMO. As would be expected given the canonical impacts of ENSO and the AMO that have been well documented in the literature (e.g., Gray 1984; Goldenberg et al. 2001), the MJO generates more normalized ACE for seven out of eight MJO index phases for both La Niña and positive AMO conditions compared with El Niño and negative AMO conditions.

One other interesting feature to note is the increase in percentage of TC activity generated in MJO index phase 4 during the course of the twentieth century, accompanied by a concomitant decrease during MJO index phase 8. While a rigorous analysis of the phase shift is beyond the scope of this paper, we speculate that this shift may be due somewhat to TC observational capabilities in the Atlantic basin. Klotzbach (2014) showed that TCs forming in the Gulf of Mexico and just off the U.S. East Coast tend to be favored in MJO index phase 8, while TC formation in the eastern Atlantic tends to be favored in MJO index phase 4. Vecchi and Knutson (2008) documented that there was very sparse ship traffic in the eastern tropical Atlantic from the late 1800s to 1965; therefore, these TCs may have been missed (or deemed to intensify later) prior to the beginning of the satellite era in the mid-1960s. Consequently, we would expect phase 8 TCs to have been better observed during the first part of the twentieth century than phase 4 TCs.

Future work will use the OT MJO index to evaluate the relationship between the MJO and TC activity in other ocean basins over multidecadal time scales (e.g., the northeastern Pacific, the northwestern Pacific, and Australia) with the obvious caveat being that other basins do not have basinwide TC records extending as far back as does the Atlantic. We will also utilize historical databases of landfall for these other basins to extend MJO–TC relationships as far back as possible. These future studies will hopefully continue to disentangle the relationships among the MJO, ENSO, and other modes of variability and TC activity.

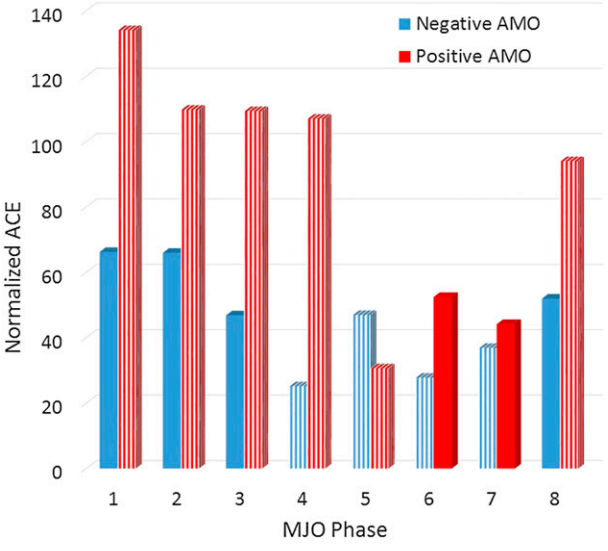

FIG. 10. As in Fig. 8, but for positive AMO years (red bars) and negative AMO years (blue bars).

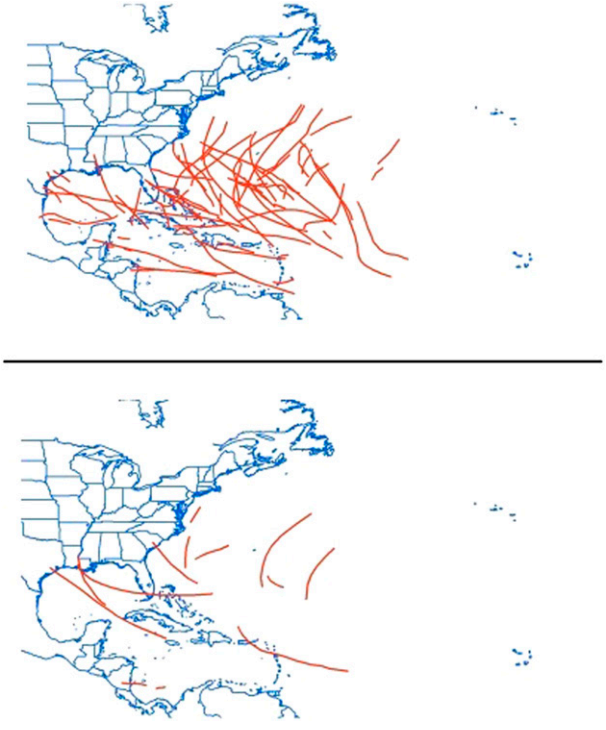

FIG. 11. As in Fig. 9, but for (top) MJO index phases 1–3 and positive AMO years and (bottom) MJO index phases 5–7 and negative AMO years.

Acknowledgments. We thank William Gray and Eric Blake for discussions on the MJO, large-scale climate modes, and their relationships with Atlantic basin TC activity. The authors would also like to acknowledge Mike Ventrice, Paul Roundy, and one unnamed reviewer for helpful comments that significantly improved the manuscript. This paper makes a contribution to the objectives of the Australian Research Council Centre of Excellence for Climate System Science (ARCCSS).

REFERENCES

Allan, R. J., and T. Ansell, 2006: A new globally complete monthly historical gridded mean sea level pressure dataset (HadSLP2): 1850–2004. *J. Climate,* **19,** 5816–5842, doi:10.1175/JCLI3937.1.

Barrett, B. S., and L. M. Leslie, 2009: Links between tropical cyclone activity and Madden–Julian oscillation phase in the North Atlantic and northeast Pacific basins. *Mon. Wea. Rev.,* **137,** 727–744, doi:10.1175/2008MWR2602.1.

Bell, G. D., and Coauthors, 2000: Climate assessment for 1999. *Bull. Amer. Meteor. Soc.,* **81,** S1–S50, doi:10.1175/1520-0477(2000)81[s1:CAF]2.0.CO;2.

Camargo, S. J., M. C. Wheeler, and A. H. Sobel, 2009: Diagnosis of the MJO modulation of tropical cyclogenesis using an empirical index. *J. Atmos. Sci.,* **66,** 3061–3074, doi:10.1175/2009JAS3101.1.

Compo, G. P., and Coauthors, 2011: The Twentieth Century Reanalysis project. *Quart. J. Roy. Meteor. Soc.,* **137,** 1–28, doi:10.1002/qj.776.

Dee, D. P., and Coauthors, 2011: The ERA-Interim reanalysis: Configuration and performance of the data assimilation system. *Quart. J. Roy. Meteor. Soc.,* **137,** doi:10.1002/qj.828.

Efron, B., 1979: Bootstrap methods: Another look at the jackknife. *Ann. Stat.,* **7,** 1–26, doi:10.1214/aos/1176344552.

Goldenberg, S. B., and L. J. Shapiro, 1996: Physical mechanisms for the association of El Niño and West African rainfall with Atlantic major hurricane activity. *J. Climate,* **9,** 1169–1187, doi:10.1175/1520-0442(1996)009<1169:PMFTAO>2.0.CO;2.

——, C. W. Landsea, A. M. Mestas-Nuñez, and W. M. Gray, 2001: The recent increase in Atlantic hurricane activity: Causes and implications. *Science,* **293,** 474–479, doi:10.1126/science.1060040.

Gray, W. M., 1968: Global view of the origin of tropical disturbances and storms. *Mon. Wea. Rev.,* **96,** 669–700, doi:10.1175/1520-0493(1968)096<0669:GVOTOO>2.0.CO;2.

——, 1979: Hurricanes: Their formation, structure and likely role in the tropical circulation. *Meteorology over Tropical Oceans,* D. B. Shaw, Ed., Royal Meteorological Society, 155–218.

——, 1984: Atlantic seasonal hurricane frequency. Part I: El Niño and 30 mb quasi-biennial oscillation influences. *Mon. Wea. Rev.,* **112,** 1649–1668, doi:10.1175/1520-0493(1984)112<1649:ASHFPI>2.0.CO;2.

Kistler, R., and Coauthors, 2001: The NCEP–NCAR 50-Year Reanalysis: Monthly means CD-ROM and documentation. *Bull. Amer. Meteor. Soc.,* **82,** 247–267, doi:10.1175/1520-0477(2001)082<0247:TNNYRM>2.3.CO;2.

Klotzbach, P. J., 2010: On the Madden–Julian oscillation–Atlantic hurricane relationship. *J. Climate,* **23,** 282–293, doi:10.1175/2009JCLI2978.1.

——, 2011: El Niño–Southern Oscillation's impact on Atlantic basin hurricanes and U.S. landfalls. *J. Climate,* **24,** 1252–1263, doi:10.1175/2010JCLI3799.1.

——, 2014: The Madden–Julian oscillation's impacts on worldwide tropical cyclone activity. *J. Climate,* **27,** 2317–2330, doi:10.1175/JCLI-D-13-00483.1.

——, and W. M. Gray, 2008: Multidecadal variability in North Atlantic tropical cyclone activity. *J. Climate,* **21,** 3929–3935, doi:10.1175/2008JCLI2162.1.

Landsea, C. W., and J. L. Franklin, 2013: Atlantic hurricane database uncertainty and presentation of a new database format. *Mon. Wea. Rev.,* **141,** 3576–3592, doi:10.1175/MWR-D-12-00254.1.

Liebmann, B., and C. A. Smith, 1996: Description of a complete (interpolated) outgoing longwave radiation dataset. *Bull. Amer. Meteor. Soc.,* **77,** 1275–1277.

Madden, R. A., and P. R. Julian, 1971: Detection of a 40-50 day oscillation in the zonal wind in the tropical Pacific. *J. Atmos. Sci.,* **28,** 702–708, doi:10.1175/1520-0469(1971)028<0702:DOADOI>2.0.CO;2.

——, and ——, 1972: Description of global-scale circulation cells in the tropics with a 40-50 day period. *J. Atmos. Sci.,* **29,** 1109–1123, doi:10.1175/1520-0469(1972)029<1109:DOGSCC>2.0.CO;2.

Maloney, E. D., and D. B. Hartmann, 2000: Modulation of hurricane activity in the Gulf of Mexico by the Madden-Julian oscillation. *Science,* **287,** 2002–2004, doi:10.1126/science.287.5460.2002.

Oliver, E. C. J., 2014: Multidecadal variations in the modulation of Alaska wintertime air temperature by the Madden–Julian Oscillation. *Theor. Appl. Climatol.,* doi:10.1007/s00704-014-1215-y, in press.

——, and K. R. Thompson, 2012: A reconstruction of Madden–Julian Oscillation variability from 1905 to 2008. *J. Climate,* **25,** 1996–2019, doi:10.1175/JCLI-D-11-00154.1.

Rasmusson, E. M., and T. H. Carpenter, 1982: Variations in tropical sea surface temperature and surface wind fields associated with the Southern Oscillation/El Niño. *Mon. Wea. Rev.,* **110,** 354–384, doi:10.1175/1520-0493(1982)110<0354:VITSST>2.0.CO;2.

Rayner, N. A., P. Brohan, D. E. Parker, C. K. Folland, J. J. Kennedy, M. Vacinek, T. J. Ansell, and S. F. B. Tett, 2006: Improved analyses of changes and uncertainties in sea surface temperature measured in situ since the mid-nineteenth century: The HadSST2 dataset. *J. Climate,* **19,** 446–469, doi:10.1175/JCLI3637.1.

Tang, B. H., and J. D. Neelin, 2004: ENSO influence on Atlantic hurricanes via tropospheric warming. *Geophys. Res. Lett.,* **31,** L24204, doi:10.1029/2004GL021072.

Vecchi, G. A., and T. R. Knutson, 2008: On estimates of North Atlantic tropical cyclone activity. *J. Climate,* **21,** 3580–3600, doi:10.1175/2008JCLI2178.1.

Ventrice, M. J., C. D. Thorncroft, and P. E. Roundy, 2011: The Madden–Julian oscillation's influence on African easterly waves and downstream tropical cyclogenesis. *Mon. Wea. Rev.,* **139,** 2704–2722, doi:10.1175/MWR-D-10-05028.1.

Wheeler, M. C., and H. H. Hendon, 2004: An all-season real-time multivariate MJO index: Development of an index for monitoring and prediction. *Mon. Wea. Rev.,* **132,** 1917–1932, doi:10.1175/1520-0493(2004)132<1917:AARMMI>2.0.CO;2.

Wolter, K., and M. S. Timlin, 1998: Measuring the strength of ENSO events—How does 1997/98 rank? *Weather,* **53,** 315–324, doi:10.1002/j.1477-8696.1998.tb06408.x.

——, and ——, 2011: El Niño/Southern Oscillation behaviour since 1871 as diagnosed in an extended multivariate ENSO index (MEI.ext). *Int. J. Climatol.,* **31,** 1074–1087, doi:10.1002/joc.2336.

Woodruff, S. D., and Coauthors, 2011: ICOADS release 2.5: Extensions and enhancements to the surface marine meteorological archive. *Int. J. Climatol.,* **31,** 951–967, doi:10.1002/joc.2103.